# Excited states and their relaxation dynamics in *trans*-polyacetylene

Jun-ichi Takimoto* and Masaki Sasai
*Institute for Molecular Science, Myodaiji, Okazaki 444, Japan*
(Received 6 September 1988)

We investigate excited states in polyacetylene, taking account of electron correlation by transforming the electronic degrees of freedom into a quantum phase variable via boson representation. When the lattice is fixed at the ground-state configuration, there are the following species of excitations: soliton $S^e$, antisoliton $\bar{S}^e$, the first breather $B_1^e$, and the second breather $B_2^e$. $S^e$ should not be confused with the usual neutral soliton $S^{e\text{-}l}$; in the former, the amount of phase change is $2\pi$ and the lattice is in the uniformly dimerized state, while in the latter the amount of phase change is $\pi$ and the lattice has a usual soliton structure. $S^e$, $B_1^e$, and $\bar{S}^e$ are three components of the triplet exciton, and $B_2^e$ is the singlet dipole-forbidden exciton which corresponds to the $2\,^1A_g$ state in finite polyenes. The electronic structure of $B_2^e$ can be regarded as a bound state of $S^{e\text{-}l}$s. We study the dynamics of the lattice relaxation from $B_2^e$ by applying a semiclassical approximation to the boson system. Since the lattice is driven by the electronic structure of $B_2^e$, a neutral soliton pair or their bound state is formed as a relaxation product.

## I. INTRODUCTION

Photoexcited states and their relaxation processes in polyacetylene have attracted much attention.[1] Especially, many experimental[1-6] and theoretical[7-14] works have been stimulated by the possibilities that various types of nonlinear excitations (solitons, polarons, or breathers[7,8]) are generated in the relaxation processes. Photoinduced absorption[2,3] and photoconduction[4] experiments show that charged solitons may be photogenerated. Photoinduced electron-spin resonance (ESR) data[6] suggest the photogeneration of neutral solitons. The 1.35-eV peak in the photoinduced absorption spectrum[1,2,5] suggests that bound states of the neutral soliton pair (breathers of diradical type[7,8]) might be generated.

On the other hand, there is now accumulating experimental evidence of the importance of the $\pi$-electron Coulomb interaction in polyacetylene,[15-19] so that one of the most important problems in photophysics of polyacetylene is to elucidate the role of the Coulomb interaction in the excited states. If the screening effect is very large and the effective Coulomb potential is very weak ($U \ll t$, where $U$ is the on-site Coulomb potential and $t$ is the transfer interaction), the Su-Schrieffer-Heeger (SSH) model which does not explicitly take account of the Coulomb interaction[20] may be a good approximation. Then, the Coulomb interaction can be treated perturbatively taking the SSH Hamiltonian as the zeroth-order starting point. If, on the other hand, the effective Coulomb interaction is not so weak ($U > t$), independent-particle picture based on the SSH model should be fundamentally altered; low-lying excitation is not a particle-hole excitation but a collective excitation.

The collective nature of the low-lying excited states is well confirmed in polyenes which are short-length-molecule versions of polyacetylene.[21] In polyenes $(CH)_n$ with $n < 22$, there is a dipole-forbidden singlet excited state in the low-energy region. This state has the same symmetry as the ground state ($A_g$ symmetry) and is 0.1–0.6 eV below the lowest dipole-allowed excited state ($B_u$ symmetry). In theoretical calculations,[21-24] a large-scale configuration-interaction (CI) expansion is necessary to make the calculated energy of this lowest $A_g$ excited state (hereafter referred to as the $2\,^1A_g$ state) lower than the energy of the lowest optically allowed $B_u$ state (the $1\,^1B_u$ state). This means that the $2\,^1A_g$ state is a collective excitation. The existence of this low-lying $2\,^1A_g$ state is evidence for the importance of the electron correlation effect in polyenes.

In *trans*-polyacetylene, the search for the corresponding dipole-forbidden excited state was done using the two-photon absorption technique by Kajzar *et al.*[25] They found the sharp two-photon absorption peak at 0.91 eV, suggesting the existence of the $^1A_g$ state at 1.82 eV, which is 0.2 eV below the peak of one-photon absorption. The existence of the low-energy $^1A_g$ state shows that the Coulomb interaction in polyacetylene is not weak; its strength is at least in the intermediate regime. Through the various theoretical methods,[26-30] many authors estimated the strength of the effective on-site Coulomb potential $U$ so as to explain the experimental data on the regularly dimerized chain and solitons. They found $U$ is about 5–6 eV; this also indicates that polyacetylene is in the intermediate correlation regime ($U > t$), and is out of the perturbative regime ($U \ll t$). In this paper, we assume the Coulomb interaction is not weak, and we mainly focus our attention on the dipole-forbidden singlet excited states in *trans*-polyacetylene. In the long chain molecule with the translational symmetry, the $2\,^1A_g$ state and other higher-energy dipole-forbidden singlet states form an exciton band. Thus we hereafter call these singlet excitations in polyacetylene the $^1A_g$ *exciton*. There are other series of dipole-forbidden states, that is, triplet excited states. The lowest energy state in this series has $B_u$ symmetry. Thus, we call this series of triplet excitations the $^3B_u$ *exciton*. For the same reason, we call the

 

low-lying optically allowed singlet excitation the $^1B_u$ *exciton.*

The physical insights on the $^1A_g$ exciton can be obtained from the theoretical analysis of the $2\,^1A_g$ state in polyenes. Using the valence-bond (VB) analysis, Soos and Ducasse[31] showed the electronic structure of the $2\,^1A_g$ state of $(CH)_8$ is very similar to that of the bound neutral soliton pair. We show in Fig. 1(a) the VB diagram corresponding to the $2\,^1A_g$ state. The $2\,^1A_g$ state of $(CH)_8$ was also analyzed by using the method of correlation function,[32] and the resemblance between the electronic structure of the $2\,^1A_g$ state and that of the neutral soliton pair was shown.[33] Ohmine *et al.*[24] used the CI expansion method based on localized orbitals. They showed that electronic configurations corresponding to the bound state of two localized triplet excitations have large weights in the CI wave function of the $2\,^1A_g$ state. We show in Fig. 1(b) some of the electronic configurations important in the CI wave function of the $2\,^1A_g$ state in $(CH)_{10}$. If we consider the localized triplet excitation in Fig. 1(b) as a bound state of two neutral solitons, then the $2\,^1A_g$ state can be regarded as a composite of four neutral solitons. Hayden and Mele[14] calculated the $2\,^1A_g$ state of $(CH)_{16}$ using the numerical renormalization-group method. They calculated optimized lattice geometry in the $2\,^1A_g$ state and showed the $2\,^1A_g$ state will relax to the neutral soliton pair in long polyenes. These investigations strongly suggest the close relationship between the $2\,^1A_g$ state and neutral soliton. The $2\,^1A_g$ state should be composed of two or four neutral solitons. In short polyenes, however, the end effect makes the physical interpretation obscure. Therefore, to prove the relation between the $^1A_g$ excitation and neutral soliton, the analysis in the longer polyene is to be desired.

The electronic structure of polyene is described by the Pariser, Parr, and Pople (PPP) Hamiltonian:

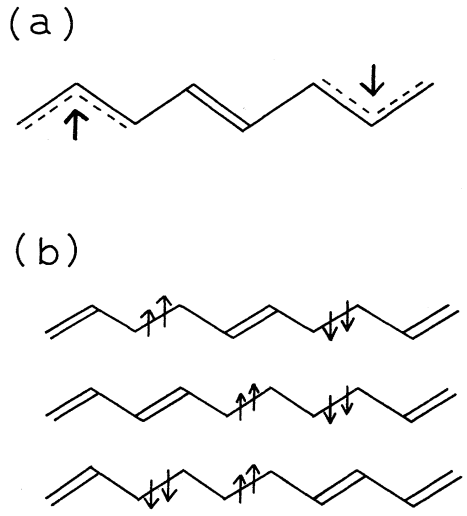


FIG. 1. (a) The VB diagram of the $2\,^1A_g$ state in $(CH)_8$, taken from Ref. 31. (b) The representative electronic configurations in the CI wave function of the $2\,^1A_g$ state in $(CH)_{10}$, taken from Table V of Ref. 24. $\uparrow\uparrow$ and $\downarrow\downarrow$ are triplet electron pairs.

$$H=\sum_{n,\sigma} t_{n,n+1}(a^{\dagger}_{n\sigma}a_{n+1\sigma}+a^{\dagger}_{n+1\sigma}a_{n\sigma}) + U\sum_n N_{n\uparrow}N_{n\downarrow}+\tfrac{1}{2}\sum_{\substack{n\neq m\\ \sigma,\sigma'}} V_{n,m}N_{n\sigma}N_{m\sigma'} + \tfrac{1}{2}\sum_n [M\dot{r}_n^2+\kappa(r_n-r_{n+1})^2]\,, \tag{1.1}$$

where $a^{\dagger}_{n\sigma}$ ($a_{n\sigma}$) is the creation (annihilation) operator of the spin up ($\sigma=\uparrow$) or down ($\sigma=\downarrow$) electron on the $n$th site, $N_{n\sigma}=a^{\dagger}_{n\sigma}a_{n\sigma}$, $t_{n,n+1}$ is the transfer integral between the $n$th and $(n+1)$st site, and $V_{n,m}$ is the Coulomb interaction between the $n$th and $m$th site. $M$ is the mass of a CH unit, $\kappa$ is the spring constant of the $\sigma$ skeleton and $r_n$ is the displacement of the $n$th C atom along the chain direction. $t_{n,n+1}$ is assumed to be linearly dependent on $(r_n-r_{n+1})$. Based on this PPP Hamiltonian, the CI methods have been applied to polyenes of lengths up to 16 carbon atoms. The CI methods, however, become increasingly difficult as the length of polyenes becomes long. Therefore, in order to discuss polyacetylene, we need to develop a different approximation suitable for the infinitely long polyene.

Since the $2\,^1A_g$ state is an almost neutral state (covalent state, in terms of the VB theory),[24,32] $^1A_g$ exciton in polyacetylene should also be a covalent excitation. A simple and natural way to describe such covalent excitations is to use the Heisenberg spin Hamiltonian

$$H=\sum_n J\left[1+\frac{\lambda}{2a}(r_n-r_{n+1})\right]\mathbf{S}_n\cdot\mathbf{S}_{n+1} + \tfrac{1}{2}\sum_n [M\dot{r}_n^2+\kappa(r_n-r_{n+1})^2]\,, \tag{1.2}$$

where $\lambda$ is an electron-lattice coupling constant and $a$ is the lattice constant. The spin Hamiltonian becomes a good approximation to the original $\pi$-electron Hamiltonian (1.1) if the Coulomb interaction is strong enough ($U\gg t$). However, even for intermediate Coulomb strength ($U>t$), the covalent excitations such as low-lying dipole-forbidden excited states can be well described by the effective spin Hamiltonian. The applicability of the spin Hamiltonian has been investigated for short polyenes; Bulaevskii[34] derived the effective spin Hamiltonian by summing up infinite perturbation series. He compared it with the PPP Hamiltonian numerically and showed that the spin Hamiltonian gives a fairly good approximation. Kuwajima[35] showed the spin Hamiltonian derived from his extended valence-bond theory agrees well with the full CI calculation in the PPP Hamiltonian. These studies indicate that the spin Hamiltonian is a good starting point to describe covalent excitations in polyacetylene.

In Sec. II, we start from the spin Hamiltonian and, using the Jordan-Wigner transformation, transform it to the Hamiltonian of spinless fermions. We first apply the mean-field (Hartree-Fock) approximation for spinless fermions and discuss the excitation spectra. We calculate how the excitation energy depends on the lattice distortion within an adiabatic approximation for the lattice degree of freedom. We will show that when the lattice is

deformed to the shape of bound solitons, the energy gap between the $2\,^1A_g$ state and the ground state becomes very small, which means that the $^1A_g$ exciton can nonradiatively decay to the ground electronic state. In Sec. III, we further transform spinless fermions to bosons using the bosonization procedure developed by Tomonaga, Luther, and others.[36] The electronic degrees of freedom are represented by a quantum phase variable. The phase Hamiltonian derived in this way was applied to polyacetylene by Nakano and Fukuyama.[37] Using this phase Hamiltonian, the electronic structure of the excited states can be described in a physically intuitive way; $^1A_g$ and $^3B_u$ excitons really have the electronic structure of bound neutral solitons even in the regularly dimerized lattice. This solitonic character of the excitons drives the lattice to generate neutral solitons. In Sec. IV, we develop the semiclassical model, which describes the dynamical lattice distortion. In Sec. V, the semiclassical equations of motion of lattice and electrons are integrated numerically and results are discussed. In Sec. VI, the photorelaxation scenario and the photogeneration of neutral solitons in polyacetylene are discussed. We also discuss the extension of the model to the more general one including both spin and charge fluctuations.

## II. EXCITATION SPECTRA IN MEAN-FIELD APPROXIMATION

Using the Jordan-Wigner transformation, spin operators in the Hamiltonian (1.2) can be transformed into spinless fermions,

$$\begin{aligned} &S_n^z=-\tfrac{1}{2}+a_n^\dagger a_n\ , \\ &S_n^+S_{n+1}^-=a_n^\dagger a_{n+1}\ , \\ &S_n^+=\exp\left[-i\pi\sum_{j=1}^{n-1}a_j^\dagger a_j\right]a_n^\dagger=(S_n^-)^\dagger\ . \end{aligned} \tag{2.1}$$

The Hamiltonian Eq. (1.2) is then expressed by spinless fermions as

$$\begin{aligned} H&=H_0+H_1+H_{\text{lattice}}\ , \\ H_0&=\tfrac{1}{2}J\sum_n[1+(-1)^n\lambda u_n/a] \\ &\quad\times(a_n^\dagger a_{n+1}+a_{n+1}^\dagger a_n-N_n-N_{n+1})\ , \\ H_1&=J\sum_n[1+(-1)^n\lambda u_n/a]N_nN_{n+1}\ , \\ H_{\text{lattice}}&=\tfrac{1}{2}\sum_n[M\dot r_n^{\,2}+\kappa(r_n-r_{n+1})^2]\ , \end{aligned} \tag{2.2}$$

where $N_n=a_n^\dagger a_n$ and $u_n$ is the order parameter for lattice distortion,

$$u_n=(-1)^n(r_n-r_{n+1})/2\ . \tag{2.3}$$

The simplest approximation to treat Hamiltonian (2.2) is the mean-field (Hartree-Fock) approximation. Within the mean-field approximation, the problem of the bond alternation in polyacetylene was discussed by Kondo[38] and excitation energy spectra in the regularly dimerized lattice were discussed by Bulaevskii[39] and by Hashimoto.[40] In this section, we calculate the $^1A_g$ excitation energy in the lattice which is distorted to the shape of bound solitons by the use of Hashimoto's method. Hashimoto showed the $2\,^1A_g$ state is expressed by the particle-hole excitation from the Hartree-Fock ground state $|\psi_{\text{HF}}\rangle$:

$$|2\,^1A_g\rangle=\frac{1}{\sqrt{2}}(a_{\text{su}}^\dagger a_{\text{ho}}-a_{\text{lu}}^\dagger a_{\text{so}})|\psi_{\text{HF}}\rangle\ , \tag{2.4}$$

where lu (ho) is the lowest unoccupied (highest occupied) Hartree-Fock orbital and su (so) is the second-lowest unoccupied (second-highest occupied) orbital. Using Eq. (2.4), we numerically calculate the energy of the singlet excited state $\langle 2\,^1A_g|H|2\,^1A_g\rangle$ for the lattice with 80 sites. The lattice is treated in the adiabatic approximation and distorted following the equation used by Onodera and Okuno.[41] Their equation for lattice structure smoothly interpolates between the regularly dimerized lattice configuration and the two-soliton configuration (soliton $S$ and antisoliton $\bar S$ are separately placed in the chain) or the four-soliton configuration ($S$, $\bar S$, $S$, and $\bar S$ are separately placed in the chain). In Fig. 2, we show how the energies of the $2\,^1A_g$ state and the ground state

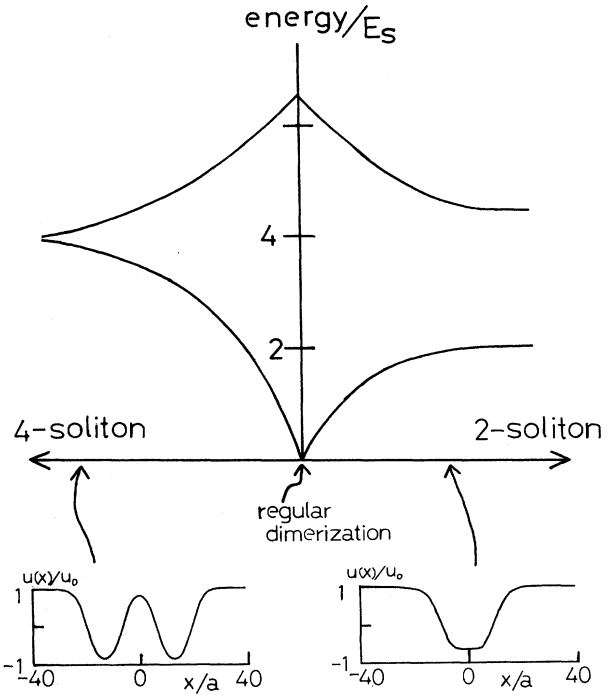


FIG. 2. The adiabatic energy spectra of the $2\,^1A_g$ state and the ground state of $(CH)_{80}$ calculated by the mean-field method using parameters $\lambda u_0/a=0.171$, $\lambda^2/(4\kappa a^2)=0.6$, and $\xi/a=4.1$, where $u_0$ is the amplitude of dimerization in the ground state and $\xi$ is soliton width. The ordinate is the energy normalized by the energy of the neutral soliton, $E_s=0.195J$. The abscissa is the lattice deformation; from the center to the right, the lattice is deformed from the regularly dimerized structure to the structure with a pair of solitons. From the center to the left, the lattice is deformed to the structure with four solitons. The lattice shapes $u(x)/u_0$ at representative points are shown in the lower part of the figure.

change when the lattice is distorted towards the two- or four-soliton configurations. Typical lattice shapes are also shown in Fig. 2. In the limit of separate $S$ and $\bar{S}$ the $2\,^1A_g$ state and the ground state are not degenerating. In the limit of a lattice with separate $S$, $\bar{S}$, $S$, and $\bar{S}$, on the other hand, the $2\,^1A_g$ state is degenerating with the ground state. The reason for this behavior is very simple. In the former limit, there are two separate doublet spins in the chain. These two isolate doublet spins can form only one singlet state, which is the ground state at this lattice configuration. Therefore, there must be a gap between the lowest two singlet states. In the latter limit, however, there are four separate doublet spins which can form two singlet states with the same energy. Thus, the mean-field method gives qualitatively correct results when the lattice is distorted to the shape of two or four separate solitons. The nonradiative transition from the $^1A_g$ excited state to the ground state is possible when the lattice has the shape of four bound solitons where the gap becomes very small.

Although the present approximation gives correct results in the above sense, there are two important deficiencies. (i) The approximation given in Eq. (2.4) describes the excited state by a particle-hole excitation from the Hartree-Fock ground state. This picture takes account of the collective nature of the excited state to some extent, since the electron correlation effect is already considered in the spin Hamiltonian (1.2). The correlation effect between spinless fermions is, however, not adequately considered. $H_1$ is not small in Eq. (2.2), so that the excited states must be treated more carefully. Therefore, quantitative details of the adiabatic energy spectrum shown in Fig. 2 are not reliable. (ii) The gap between the singlet excited state and the ground state becomes very small when the lattice begins to have the shape of bound solitons. Then the adiabatic approximation does not hold and the nonadiabatic treatment of the lattice becomes necessary. To overcome the first point, we use, in Sec. III, the method of boson representation. The boson method gives a clear picture for the excited states. The second point, the nonadiabaticity, is taken into account by the semiclassical method introduced in Sec. IV.

## III. ELECTRONIC STRUCTURE OF $^1A_g$ AND $^3B_u$ EXCITONS

In order to treat the strongly interacting spinless fermions, we employ the method of the boson representation developed by Tomonaga, Luther, and others.[36] The boson method was applied to polyacetylene by Nakano and Fukuyama.[37] They showed that in the continuum limit $a\to 0$, the Hamiltonian (2.2) for the spinless fermion can be transformed into the Hamiltonian for the phase boson:

$$H=\int dx\,\{A\,[\nabla\hat{\phi}(x)]^2-B(x)\cos\hat{\phi}(x)+C\hat{\pi}(x)^2 +(M/2a)\dot{u}(x)^2+(2\kappa/a)u(x)^2\}\ , \tag{3.1a}$$

where

$$A=Ja/8\ ,\quad B(x)=\lambda Ju(x)/a^2\ ,\quad C=\pi^2Ja/2\ , \tag{3.1b}$$

and $u(x)$ is defined as $u(x=na)=u_n$. $\hat{\phi}(x)$ is a boson operator and $\hat{\pi}(x)$ is its conjugate momentum operator satisfying $[\hat{\phi}(x),\hat{\pi}(x')]=i\delta(x-x')$. $A$ and $C$ are determined so that the Hamiltonian (3.1) reproduces the exact results for the spin wave velocity and the correlation function in the case $u(x)=0$.[42] The phase $\hat{\phi}$ is related to the local spin density $\hat{m}(x)$ by the following equation:

$$\hat{m}(x)=\frac{1}{2\pi}\nabla\hat{\phi}+\frac{1}{a}\sin[2k_Fx+\hat{\phi}(x)]\ , \tag{3.2}$$

where $k_F$ is the Fermi wave number $\pi/2a$. The spin density at the $n$th site of the original electron system is $\hat{m}(x=na)$.

The ground state of the Hamiltonian Eq. (3.1) is determined by the self-consistent harmonic approximation (SCHA).[37] The amplitude of dimerization $u_0$ and the quantum fluctuation $\langle\hat{\phi}^2\rangle$ in the ground state is given, within the SCHA, by

$$u_0/a=\frac{\lambda^2}{\pi}\left[\frac{J}{4\kappa a^2}\right]^{3/2}\ , \tag{3.3}$$

$$e^{-\langle\hat{\phi}^2\rangle/2}=\left[\frac{\lambda u_0}{\pi^2 a}\right]^{1/3}\ . \tag{3.4}$$

Using the identity

$$\cos\hat{\phi}=e^{-\langle\hat{\phi}^2\rangle/2}{:}\cos\hat{\phi}{:}\ , \tag{3.5}$$

where : : means the normal ordering with respect to the ground state determined by the SCHA, we can express the Hamiltonian Eq. (3.1) in the following form:

$$H=\frac{v}{\beta^2}\int dx\left[\frac{1}{2}[\nabla\hat{\phi}(x)]^2+\tfrac{1}{2}\beta^4\hat{\pi}(x)^2 -q_0^2Q(x)[{:}\cos\hat{\phi}(x){:}] +\tfrac{1}{2}q_0^2\left[Q(x)^2+\frac{1}{\omega^2}\dot{Q}(x)^2\right]\right]\ , \tag{3.6a}$$

where

$$\beta^2=(C/A)^{1/2}=2\pi\ ,\quad v=2(AC)^{1/2}=\pi Ja/2\ ,\quad q_0^2=\beta^2(\lambda Ju_0/a^2v)e^{-\langle\hat{\phi}^2\rangle/2}\ ,\quad Q(x)=u(x)/u_0\ ,\quad \omega=(4\kappa/M)^{1/2}\ . \tag{3.6b}$$

Here $\beta^2$ is the parameter which represents the strength of the quantum fluctuation and plays the role of $\hbar$ in the semiclassical expansion.[43]

In this section, we discuss the electronic structure in the static lattice $\dot{Q}(x)=0$. First we study the neutral soliton by expressing the boson state by the coherent state

$$|\phi_c\pi_c\rangle=e^{iG(\phi_c\pi_c)}|0\rangle\ , \tag{3.7}$$

$$G(\phi_c\pi_c)=\int[\beta^{-2}\pi_c(x)\hat{\phi}(x)-\phi_c(x)\hat{\pi}(x)]dx\ . \tag{3.8}$$

Here $|0\rangle$ is the ground state at $u(x)=u_0$. $\phi_c$ and $\pi_c$ are

real $c$-number functions which have the meaning of the expectation values of $\hat{\phi}(x)$ and $\hat{\pi}(x)$:

$$\langle \phi_c \pi_c | \hat{\phi}(x) | \phi_c \pi_c \rangle = \phi_c(x) ,$$
$$\langle \phi_c \pi_c | \hat{\pi}(x) | \phi_c \pi_c \rangle = \beta^{-2} \pi_c(x) . \tag{3.9}$$

$\beta^{-2}$ is introduced in front of $\pi_c$ so that both $\phi_c$ and $\pi_c$ become of order $\beta^0$. The energy expectation value is

$$E_c = \langle \phi_c \pi_c | H | \phi_c \pi_c \rangle$$
$$= \frac{v}{\beta^2} \int dx \left[ \tfrac{1}{2} (\nabla \phi_c)^2 + \tfrac{1}{2} \pi_c^2 - q_0^2 Q \cos\phi_c + \tfrac{1}{2} q_0^2 Q^2 \right] . \tag{3.10}$$

The expectation value of the spin density is given by

$$m(x) = \langle \phi_c \pi_c | \hat{m}(x) | \phi_c \pi_c \rangle$$
$$= \frac{1}{2\pi} \nabla \phi_c(x) + \frac{1}{a} e^{-\langle \hat{\phi}^2 \rangle / 2} \cos(2k_F x) \sin\phi_c(x) , \tag{3.11}$$

in which a term containing $\sin(2k_F x)$ is dropped since $\sin(2k_F x) = 0$ at the lattice site $x = na$. Minimizing $E_c$ with respect to $\phi_c(x)$, $\pi_c(x)$, and $Q(x)$ under the boundary condition $Q(\pm\infty) = \pm 1$, we get $\pi_c(x) = 0$ and

$$\cos\phi_c(x) = \tanh(x/\xi) , \tag{3.12}$$

$$Q(x) = \cos\phi_c(x) , \tag{3.13}$$

where

$$\xi = 1/q_0 . \tag{3.14}$$

$\phi_c(x)$ and $m(x)$ of this neutral soliton are shown in Fig. 3(a). The formation energy of the neutral soliton is, using Eq. (3.10),

$$E_s = 2/(\beta^2 \tau_0) = 1/(\pi \tau_0) , \tag{3.15}$$

where

$$\tau_0 = \xi / v . \tag{3.16}$$

Nakano and Fukuyama included quantum correction to this energy and found $E_s = 1.81/(\beta^2 \tau_0)$.

We next consider $^1A_g$ and $^3B_u$ excitons in the uniform-

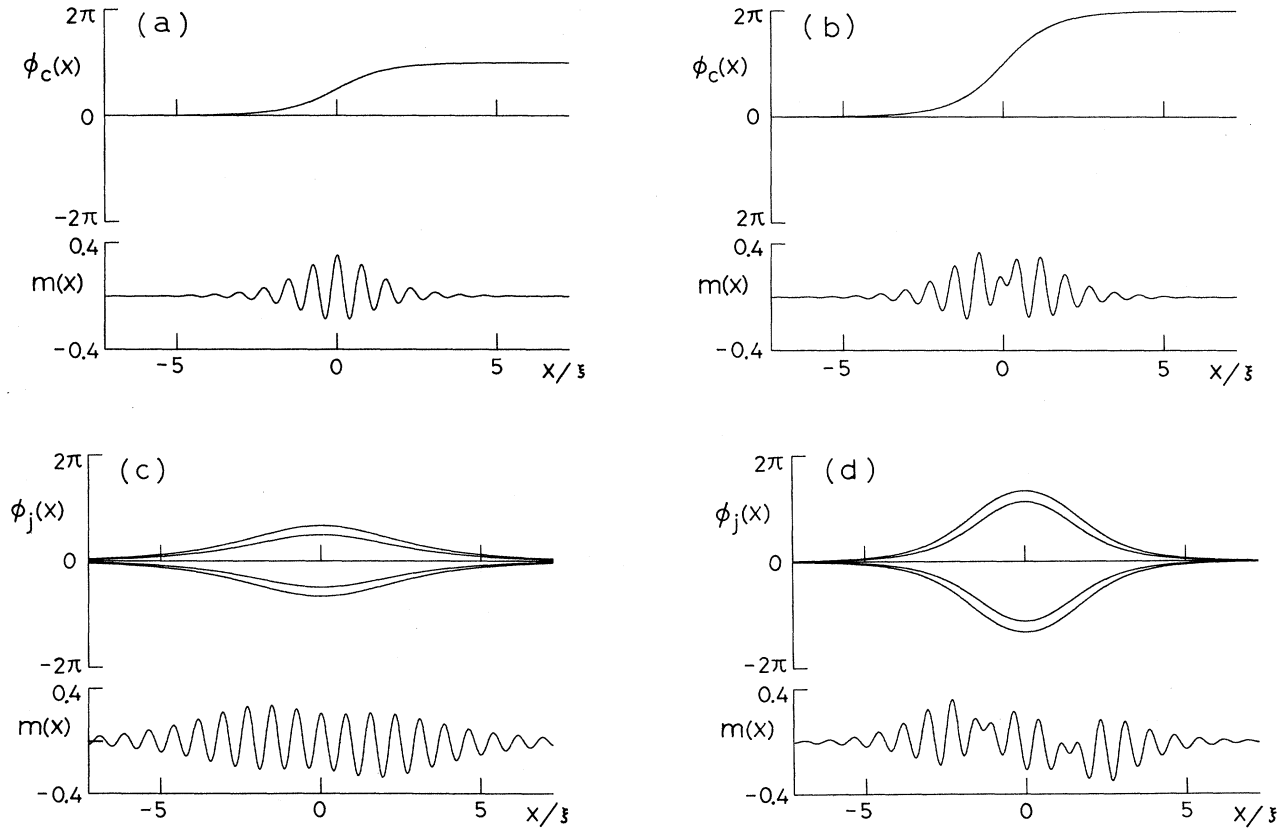


FIG. 3. Internal structure $\phi_c(x)$ and the corresponding spin density $m(x)$ [defined in Eq. (3.11)] of (a) neutral soliton $S^{e\text{-}l}$, (b) electronic soliton $S^e$, (c) first electronic breather $B_1^e$, and (d) second electronic breather $B_2^e$. In the case of (c) and (d), we showed $\phi_j(x) = \phi(\chi_j; x, t=0)$ with $\chi_j = 2\pi j/8$ ($j = -2, -1, 0, 1, 2$) and $m(x)$ corresponding to $\phi_{j=2}(x)$.

ly dimerized lattice. When the lattice is fixed as $Q(x)=1$, Eq. (3.6a) becomes a well-known sine-Gordon Hamiltonian. Its excitation spectrum is studied by Dashen *et al.*[43] (DHN) using the semiclassical path-integral method. The procedure of DHN is summarized as follows. They first find all the static or periodic solutions of the classical equation of motion

$$\ddot{\phi}_c(x)=v\dot{\pi}_c(x)=v^2(\nabla^2\phi_c-q_0^2\sin\phi_c)\ . \tag{3.17}$$

Then these classical solutions are quantized using the semiclassical quantization condition. Finally, the effect of the small quantum fluctuation around the classical solutions is taken into account by the simple renormalization of the parameter $\beta$; i.e., $\beta^2$ is replaced by $\beta'^2=\beta^2/(1-\beta^2/8\pi)=8\pi/3$.

The classical equation of motion has two kinds of solutions: one is the soliton solution, which is a static solution; the other is the breather solution, which is a periodic solution. Through the quantization method described above, the soliton solution becomes a quantum-mechanical particle with energy

$$E_0=8/(\beta'^2\tau_0)\ . \tag{3.18}$$

The corresponding classical solution is

$$\begin{aligned}&\phi_c(x)=4\tan^{-1}[\exp(x/\xi)]\ ,\\ &\pi_c(x)=0\ .\end{aligned} \tag{3.19}$$

The amount of phase change accompanying this soliton and the neutral soliton of Eq. (3.12) is $2\pi$ and $\pi$, respectively. In order to avoid confusion, we call the soliton of Eq. (3.19) "electronic soliton" $S^e$, and the neutral soliton "electron-lattice soliton" $S^{e\text{-}l}$, since the former is a pure electronic excitation in the uniformly dimerized lattice.

Among the classical breather solutions with various oscillation frequencies, only the solutions with frequencies

$$\omega_n=\tau_0^{-1}\cos(n\beta'^2/16) \tag{3.20}$$

are selected by the quantization condition. Here the quantum number $n$ can take the values $n=1,2,\ldots,<8\pi/\beta'^2$. The energy of this quantized breather is

$$E_n=(16/\beta'^2\tau_0)\sin(n\beta'^2/16)\ . \tag{3.21}$$

Its corresponding classical solution is

$$\begin{aligned}\phi_c(\chi;x,t)&=4\tan^{-1}\left[\tan(n\beta'^2/16)\right.\\ &\quad\left.\times\frac{\sin(\omega_n t+\chi)}{\cosh[\sin(n\beta'^2/16)(x/\xi)]}\right],\\ \pi_c(\chi;x,t)&=\dot{\phi}_c/v\ ,\end{aligned} \tag{3.22}$$

where $\chi$ is the initial phase of the oscillation. Equations (3.18) and (3.21) are believed to be exact although their derivation is approximate.[43] These energies correspond to the excitations with zero translational momentum. Since the sine-Gordon Hamiltonian has Lorentz invariance, the energy of the excitation with finite momentum $p$ is given by

$$\varepsilon(p)=(v^2p^2+\varepsilon_0^2)^{1/2}\ , \tag{3.23}$$

where $\varepsilon_0$ is given by Eq. (3.18) or (3.21).

Since $\beta'^2=8\pi/3$ in the present case, there are only two quantized breathers ($n=1$ or 2). We will refer to the breather with $n=1$ (2) as the first (second) electronic breather $B_1^e$ ($B_2^e$), in order to avoid the confusion with the electron-lattice breather $B^{e\text{-}l}$ previously discussed in Refs. 7 and 8. Equations (3.18) and (3.21) show that $E_1=E_0$, i.e., the energy of $B_1^e$ is equal to that of $S^e$. The energy of $B_2^e$ is $E_2=\sqrt{3}E_0$. Since the $z$ component of the total spin $\int m(x)dx$ of $S^e$, $B_1^e$, and $\bar{S}^e$ is 1, 0, and $-1$, respectively, these three excitations should correspond to the three components of the triplet exciton ($^3B_u$ exciton). The remaining excitation $B_2^e$ corresponds to the $^1A_g$ exciton. If we use Nakano and Fukuyama's parameters[37] $J=2$ eV, $\lambda=8.1$, and $\kappa a^2=55$ eV, $\xi$ and $\tau_0$ can be estimated, using Eqs. (3.3), (3.6b), (3.14), and (3.16), to be $\xi=2.6a$ and $\tau_0=0.55$ fsec. Then the energy of the $^3B_u$ exciton is $E_0=1.1$ eV and the energy of the $^1A_g$ exciton is $E_2=2.0$ eV. $E_2$ well reproduces the value 1.82 eV of the two-photon absorption peak.[25]

The state vectors of these excitons can be constructed, within the semiclassical approximation, by superposing the coherent states Eq. (3.7) as follows. For $S^e$, it is given by

$$\begin{aligned}&|S^e\rangle=\int dz\, f(z)|z\rangle\ ,\\ &|z\rangle=e^{-i\hat{P}z}|\phi_c\pi_c\rangle\ ,\end{aligned} \tag{3.24a}$$

where

$$\hat{P}=-\int dx[\nabla\hat{\phi}(x)]\hat{\pi}(x) \tag{3.25}$$

is the translational momentum operator and $\exp(-i\hat{P}z)$ is the spatial displacement operator. Equation (3.19) should be used for $\phi_c$ and $\pi_c$. $f(z)$ is a complex $c$-number function, and it should be a plane wave $\exp(ipz)$ in order for $|S^e\rangle$ to be an eigenstate of $\hat{P}$. In the case of $B_n^e$, on the other hand, states at various oscillation phase $\chi$ must also be superposed,

$$\begin{aligned}&|B_n^e\rangle=\int dz\,d\chi\, f(z,\chi)|z,\chi\rangle\ ,\\ &|z,\chi\rangle=e^{-i\hat{P}z}|\phi_c(\chi;x,0)\pi_c(\chi;x,0)\rangle\ ,\end{aligned} \tag{3.24b}$$

in which Eq. (3.22) should be used for $\phi_c$ and $\pi_c$.

In order to visualize the internal structure of these excitons, we show in Figs. 3(b)–3(d) the classical solution $\phi_c(x)$ and the corresponding spin density $m(x)$ [Eq. (3.11)] of $S^e$ and $B_n^e$ ($n=1,2$). In the case of $B_n^e$ we show snapshots of oscillating $\phi_c$, together with $m(x)$ corresponding to the $\phi_c$ with maximum amplitude. By comparing Figs. 3(b) and 3(c) with Fig. 3(a), we see that the electronic structure of $S^e$ or $B_1^e$ can be regarded as a bound state of two $S^{e\text{-}l}$s. On the other hand, Fig. 3(d) indicates that the electronic structure of $B_2^e$ can be interpreted either as a bound state of $S^e$ and $\bar{S}^e$ or as a bound state of two or more $S^{e\text{-}l}$s. This interpretation is in agreement with the analyses of the structure of the $2\,^1A_g$ state in finite polyenes[24,31,33] which were discussed in the Introduction.

## IV. METHOD OF SIMULATION OF RELAXATION DYNAMICS

In this and following sections, we get rid of the restriction $\dot{Q}(x)=0$ and study the relaxation dynamics of excited states. In order to follow these dynamics, we must determine the time dependence of the lattice order parameter $Q(x,t)$ and of the state vector of the boson system $|\Psi(t)\rangle$. We treat $Q(x,t)$ as a classical variable and determine its time dependence by

$$\ddot{Q}(x,t)=-\omega^2[Q(x,t) - \langle\Psi(t)|:\cos\hat{\phi}(x):|\Psi(t)\rangle/\langle\Psi(t)|\Psi(t)\rangle] . \tag{4.1}$$

As the state vector $|\Psi(t)\rangle$ we use the superposition of coherent states Eq. (3.24), in which $\phi_c$, $\pi_c$, and $f$ are taken to be time-dependent functions. First we consider the relaxation of electronic soliton $|S^e\rangle$. In this case we assume that $|\Psi(t)\rangle$ always has the form of Eq. (3.24a). At $t=0$, $\phi_c$ and $\pi_c$ are given by Eq. (3.19) and $f(z)$ is taken to be a sufficiently delocalized wave packet. We determine the time dependence of these functions by the time-dependent variational principle

$$\frac{d}{dt}\frac{\delta\mathcal{L}}{\delta\dot{\phi}_c(x)}=\frac{\delta\mathcal{L}}{\delta\phi_c(x)} , \tag{4.2}$$

where

$$\mathcal{L}=\frac{1}{\langle\Psi|\Psi\rangle}\left[\frac{i}{2}(\langle\Psi|\dot{\Psi}\rangle-\langle\dot{\Psi}|\Psi\rangle)-\langle\Psi|H|\Psi\rangle\right] , \tag{4.3}$$

and similar equations for $\pi_c$ and $f(z)$. (Note that $\pi_c$ is not the momentum conjugate to $\phi_c$; both of them are generalized coordinates in the Lagrangian formalism.) Although the Lagrangian $\mathcal{L}$ can be evaluated exactly, the resultant equations of motion are too complicated to be handled. To simplify the form of $\mathcal{L}$ we use the Gaussian overlap approximation (GOA),[44] which is a kind of semiclassical (small-$\beta^2$) approximation. Details of this approximation are given in Appendix. The final result for $\mathcal{L}$ is

$$\mathcal{L}=\frac{i}{2}\int dz[g^*(z)\dot{g}(z)-\dot{g}^*(z)g(z)] - \int dz\, g^*(z)\mathcal{H}_{\rm eff}g(z) , \tag{4.4}$$

where $\mathcal{H}_{\rm eff}$ is given by Eq. (A33) and $g(z)$ is defined by Eq. (A15). Due to the nonzero overlap $\langle z_1|z_2\rangle$ for $z_1\neq z_2$, not $f(z)$ but $g(z)$ should be interpreted as a wave function of the center of mass of the excitation. Note that $g(z)$ is always normalized: $\int dz|g(z)|^2=1$. The equation of motion of $g(z)$ is

$$\begin{aligned} i\dot{g}(z)&=\mathcal{H}_{\rm eff}g(z) \\ &=-\partial A(z)\partial g(z)-i[W'(z)+2W(z)\partial]g(z) \\ &\quad +V(z)g(z) , \end{aligned} \tag{4.5}$$

where $\partial=\partial/\partial z$ and $W(z)$ is given by Eq. (A20). $A(z)$ and $V(z)$ are given by Eqs. (A34) and (A35), respectively. $V(z)$ acts as a potential for $g(z)$, and $A(z)$ plays the role of the inverse mass. If we derive the equations of motion of $\phi_c$ and $\pi_c$ using Eq. (4.4), the resultant equations are still very complicated. But neglecting terms of higher order in $\beta^2$, we get

$$\begin{aligned} &v^{-1}\dot{\phi}_c(x)=\pi_c(x) , \\ &v^{-1}\dot{\pi}_c(x)=\phi_c''(x)-q_0^2\sin\phi_c(x)\int dz|g(z)|^2Q(x+z) . \end{aligned} \tag{4.6}$$

In a similar way, the equation of motion for $Q$ is given by

$$\omega^{-2}\ddot{Q}(x)=-Q(x)+\int dz|g(z)|^2\cos\phi_c(x-z) . \tag{4.7}$$

If we include terms higher order in $\beta^2$ into Eqs. (4.6) and (4.7), the energy expectation value $E$ [given in Eq. (A17)] would be strictly conserved. Actually, we retained only the lowest-order terms in Eqs. (4.6) and (4.7) and $E$ is not strictly conserved. But the results of numerical calculations using Eqs. (4.5)–(4.7) show that $E$ fluctuates only about 10%. This fact partially justifies the neglect of higher-order terms.

Numerical simulation of Eqs. (4.5)–(4.7) is carried out by usual discretization method using spatial and time steps $\Delta x=(0.1-0.2)\xi$ and $\Delta t=(0.001-0.005)\tau_0$.

Within the framework of the semiclassical approximation, it would be natural to assume that $g(z)$ is of Gaussian form:

$$g(z)=(2\alpha_R/\pi)^{1/4}e^{-\alpha z^2} , \tag{4.8}$$

$$\alpha=\alpha_R+i\alpha_I . \tag{4.9}$$

In this approximation, Eq. (4.5) is replaced by the equations of motion of $\alpha_R$ and $\alpha_I$. The latter equations are easily obtained by first expressing $\mathcal{L}$ in terms $\alpha_R$ and $\alpha_I$, and then using the Euler equation

$$\frac{d}{dt}\frac{\partial\mathcal{L}}{\partial\dot{\alpha}}=\frac{\partial\mathcal{L}}{\partial\alpha} . \tag{4.10}$$

We carried out two types of simulations using Eqs. (4.5) and (4.10), and got similar results.

So far we considered the relaxation of the electronic soliton $S^e$. Next we consider the relaxation of the electronic breather $B_n^e$. In this case, the initial condition for $|\Psi(t)\rangle$ should be of the form of Eq. (3.24b), i.e., we must average over the initial phase $\chi$. Since we cannot keep track of infinitely many values of $\chi$, we discretize in the $\chi$ direction and approximate $|\Psi(t)\rangle$ in the following form:

$$|\Psi(t)\rangle=\frac{1}{(N_B)^{1/2}}\sum_{j=1}^{N_B}\int dz\, f(z)|z,j\rangle , \tag{4.11}$$

where $|z,j\rangle=e^{-i\hat{P}z}|\phi_j\pi_j\rangle$, and $|\phi_j\pi_j\rangle$ is given by Eq. (3.7) in which $\phi_c$ and $\pi_c$ are replaced by $\phi_j$ and $\pi_j$. At $t=0$, $\phi_j$ and $\pi_j$ are given by Eq. (3.22) with $\chi$ equal to

$$\chi_j=2\pi j/N_B, \quad j=1,2,\ldots,N_B . \tag{4.12}$$

In the actual calculations we take $N_B=8$ or 16. In the spirit of the semiclassical approximation, we assume that

$$\langle z_1,j_1|\cdots|z_2,j_2\rangle\simeq 0 \quad (j_1\neq j_2) . \tag{4.13}$$

Within this approximation, the evaluation of $\mathcal{L}$ in terms

of $\phi_j$, $\pi_j$, $g(z)$, and $Q(z)$ is almost identical to that in the soliton case. If we denote the Lagrangian in the soliton case [Eq. (4.4)] by $\mathcal{L}_{\text{soliton}}(\phi_c,\pi_c)$, the Lagrangian in the breather case is given by

$$\mathcal{L}_{\text{breather}}=\frac{1}{N_B}\sum_{j=1}^{N_B}\mathcal{L}_{\text{soliton}}(\phi_j,\pi_j)\ . \tag{4.14}$$

The resultant equations of motion are also very similar to those in the soliton case. Equations for $\phi_j$ and $\pi_j$ are identical to Eqs. (4.6). Equations for different values of $j$ are decoupled. Equations for $g(z)$ and $Q(x)$ are given by Eqs. (4.5) and (4.7) except that the terms containing $\phi_c$ and $\pi_c$ are replaced by the average over $j$ of the form of Eq. (4.14). For example, Eq. (4.7) is replaced by

$$\omega^{-2}\ddot{Q}(x)=-Q(x)+\int dz\,|g(z)|^2\frac{1}{N_B}\sum_{j=1}^{N_B}\cos\phi_j(x-z)\ . \tag{4.15}$$

In the actual simulations we take $\xi$ and $\tau_0$ as a unit of length and time, respectively. If we express the equations of motion in terms of the dimensionless variables $\tilde{x}=x/\xi$ and $\tilde{t}=t/\tau_0$, all of the parameters with dimension disappear from the equations and only two dimensionless parameters remain: $\beta^2$ and $\omega\tau_0$. Although $D(x)$ defined in Eq. (A3) depends on the cutoff wave number $k_c$, actual dynamics do not depend on this cutoff (or on $\xi/a$). The reason is that $D(x)$ itself is irrelevant and only integrals of $D(x)$ [such as $\eta(x)$ defined in Eq. (A22)] are relevant to dynamics. These integrals have finite values even in the limit $k_c\to\infty$, as long as $\phi_c(x)$ and $\pi_c(x)$ are well-behaved functions. Thus the dynamics do not depend on $k_c$ as long as $k_c\xi\gg1$. Since we fix $\beta^2$ at $2\pi$, $\omega\tau_0$ is the only parameter of our simulations.

## V. RESULTS OF THE SIMULATIONS

We first discuss the initial conditions of our simulations. At $t=0$ the lattice is taken to be in the uniformly dimerized state: $Q(x,t=0)=1$ and $\dot{Q}(x,t=0)=0$. $|\Psi(t=0)\rangle$ is assumed to be either the electronic soliton $|S^e\rangle$ or the electronic breather $|B_n^e\rangle$. $g(z,t=0)$ is taken to be a sufficiently delocalized wave packet. Some comments on this initial condition for $g(z)$ are necessary.

If the $^1A_g$ exciton, for example, is created by a two-photon absorption, its center of mass may be in a delocalized (plane-wave) state. But if we take a plane-wave state as an initial condition for $g(z)$, the lattice order parameter $Q(x)$ is under uniform and infinitesimally small force, and no lattice relaxation will take place. This is a shortcoming of the classical treatment of $Q(x)$. If we treat $Q(x)$ quantum mechanically, lattice relaxations can take place even if we start from a translationally invariant state. Although the state vector [including that for $Q(x)$] has a translational invariance at all times, it would be, after the relaxation completes, a superposition of wave packets which are localized at various positions along the chain. In other words, translational invariance can be broken through the quantum fluctuation of $Q(x)$. In our classical treatment of $Q(x)$ this localization process cannot be described.

We avoid this difficulty by using as an initial condition for $g(z)$ not a plane-wave state but a wave packet localized within a large but finite region. More explicitly, we take $g(z,t=0)$ to be of the form of Eq. (4.8) with $\alpha_R=(10^{-2}-10^{-3})\xi^{-2}$. The corresponding width $\sigma$ of the Gaussian $|g(z)|^2$, defined by

$$\sigma=\tfrac{1}{2}\alpha_R^{-1/2}\ , \tag{5.1}$$

is $(5-16)\xi$. This assumption may seem rather arbitrary at first. In real polyacetylene samples, however, there are many inhomogeneities due to, for example, the thermal fluctuation of $Q(x)$, finiteness of the chain length, various lattice imperfections, etc. These inhomogeneities would cause the localization of $g(z)$. Thus the above assumption for $g(z,t=0)$ is, in our opinion, an acceptable one.

Now we present the results of the simulations. We focus on the relaxation of $B_2^e$, which corresponds to the $^1A_g$ exciton. First we show the results of a simulation using Eq. (4.10); $g(z)$ is taken to be of the form of Eq. (4.8) at all $t$. The initial condition for $\alpha$ is taken to be $\alpha_R=10^{-3}\xi^{-2}$ and $\alpha_I=0$. $|\Psi(t)\rangle$ is assumed to be of the form of Eq. (4.11) with $N_B=8$. The total length $L$ of the system is taken to be $L=60\xi$, and the periodic boundary condition is used. The frequency of the lattice vibration $\omega$ is set to $0.2\tau_0^{-1}$. The equations of motion are discretized using spatial and time steps $\Delta x=0.2\xi$ and $\Delta t=0.005\tau_0$. Figure 4 shows the time dependence of the width $\sigma$ of the Gaussian $|g(z)|^2$ defined in Eq. (5.1). The actual forms of $|g(x)|^2$ at typical instances are shown in Fig. 5, together with the forms of $Q(x)$. Since $\phi_j$ has a form of bound neutral solitons, the lattice starts to be deformed to the shape of the soliton pair following Eq. (4.15). Then the deformed lattice gives rise to the attractive potential $V(z)$ [see Eq. (A21)]. $g(z)$ starts to localize due to this potential $V(z)$, and the localized $g(z)$ gives the stronger force for the lattice deformation. Thus, the relaxation process proceeds in a cooperative way and the lattice is deformed to the form of the soliton pair. The solitonic shape of $\phi_j$ is the driving force of the whole process. The actual dynamics, however, does not proceed in

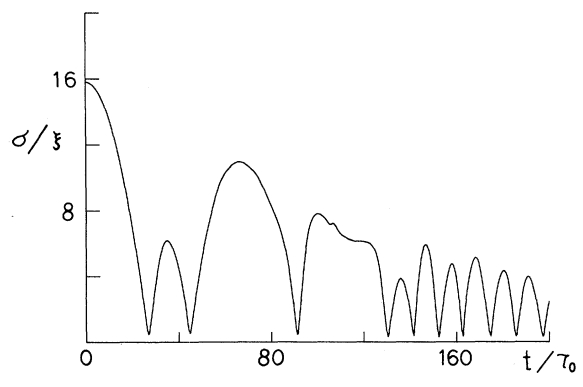


FIG. 4. The time dependence of the width $\sigma$ of the wave packet $|g(x)|^2$. Gaussian approximation Eq. (4.11) is used for $g(z)$. The frequency of the lattice vibration $\omega=0.2\tau_0^{-1}$.

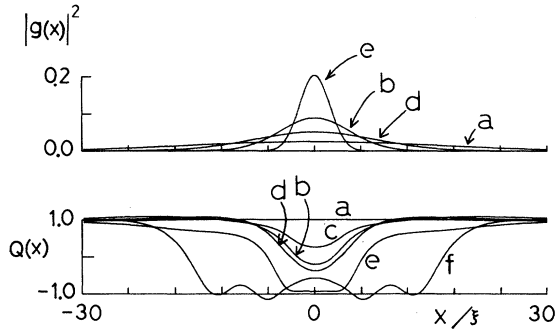


FIG. 5. The probability amplitude $|g(x)|^2$ of the center of mass of the excitation and the lattice order parameter $Q(x)$ at several typical $t$. (a) $t=0$, (b) $t=40\tau_0$, (c) $t=60\tau_0$, (d) $t=100\tau_0$, (e) $t=140\ \tau_0$, and (f) $t=180\tau_0$.

such a straightforward way. As can be seen from Fig. 4, at $t\simeq 30\tau_0$, $g(z)$ begins to delocalize again without waiting for the lattice motion. This is due to the large kinetic energy of $g(z)$ motion. Then the force acting on $Q(x)$ becomes weak and $Q(x)$ returns to the initial configuration $Q(x)=1$, although $Q(x)$ cannot follow the motion of $g(z)$ completely. Thus from $t=30\tau_0$ to $100\tau_0$, $g(z)$ and $Q(x)$ show complicated oscillations. But the lattice is eventually deformed to the shape of the soliton pair for $t>120\tau_0$. The generated neutral solitons are running away from each other. The oscillation of $g(z)$ is left even for $t>140\tau_0$. In Fig. 6 we show internal structures of the excitation $\phi_j(x)(j=1,2,\ldots,N_B=8)$. Up to $t=(100-120)\tau_0$ their motion is similar to that of the electronic breather [see Eq. (3.22)]; they oscillate with a period close to $2\pi/\omega_2=4\pi\tau_0\simeq 13\tau_0$ [$\omega_2$ is defined in Eq. (3.20)]. At around $t=(100-120)\tau_0$ they stop oscillating and rapidly approach to the soliton-pair form. Since we started from a singlet state, the resultant soliton pair is a singlet linear combination of $S_{\uparrow}^{e\text{-}l}+S_{\downarrow}^{e\text{-}l}$ and $S_{\downarrow}^{e\text{-}l}+S_{\uparrow}^{e\text{-}l}$.

Next we show the result of a simulation using Eq. (4.5). We used the parameters $L=60\xi$, $\Delta x=0.1\xi$, $\Delta t=0.001\tau_0$, $\omega\tau_0=0.1$, and $N_B=16$. The initial condition for $g(x)$ is given by Eq. (4.8) with $\alpha_R=0.01\xi^{-2}$ and $\alpha_I=0$. Figure 7 shows the forms of $|g(x)|^2$ and $Q(x)$ at several typical $t$. As can be seen, $g(x)$ is almost always Gaussian-like; the Gaussian approximation for $g(x)$ was a reasonable one. The oscillation of the width of the wave packet $|g(x)|^2$ still exists in this more accurate treatment of $g(x)$, although it cannot be seen from the data shown in Fig. 7 alone. $Q(x)$ in Fig. 7, on the other hand, smoothly approaches the soliton-pair form with no oscillation, unlike in Fig. 5. The reason for this difference is that in Fig. 7, compared with Figs. 4–6, the initial value of $\alpha_R$ is larger and $\omega$ is smaller. With the larger value of $\alpha_R(t=0)$ the amplitude of the oscillation of $g(x)$ is reduced: with the smaller value of $\omega$ the motion of $Q(x)$ becomes slower and it experiences time-averaged force from $g(x)$. Thus the oscillation of $g(x)$ has weaker effects on the motion of $Q(x)$, and $Q(x)$ changes smoothly into the soliton-pair form. The motion of $\phi_j(x)$ is similar to that in Fig. 6 and not shown here.

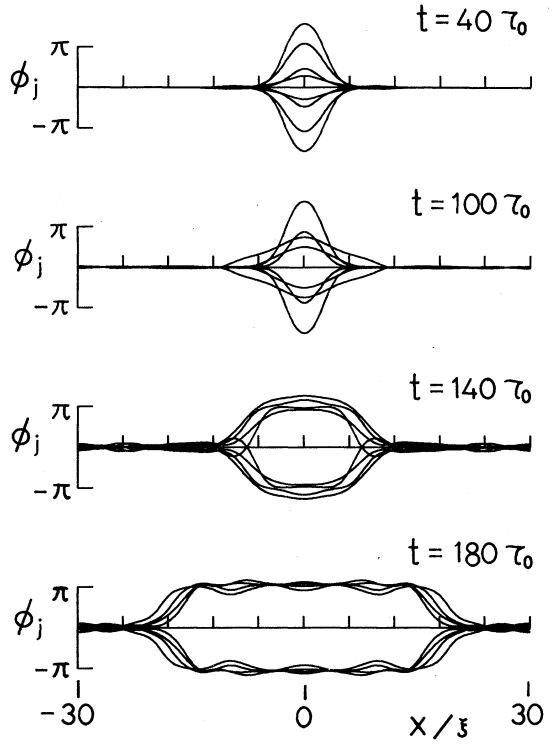


FIG. 6. Internal structures $\phi_j(x)$ $(j=1-8)$ of the excitation at $t=40\tau_0$, $100\tau_0$, $140\tau_0$, and $180\tau_0$.

In both of the above two examples the final state was the neutral soliton pair. If the initial width of $g(z)$ is sufficiently small [$\sigma(0)/\xi<2-5$], we always get the soliton pair as a final state. If, however, we increase the initial width of $g(z)$, the probability of getting the soliton pair decreases. (This probability also decreases if we increase $\omega$.) When the soliton pair is not formed, what we get is a localized large-amplitude oscillation of $Q(x)$. This kind of oscillation has been previously studied within an adiabatic approximation.[7,8] In this approximation the electronic state completely follows the motion of

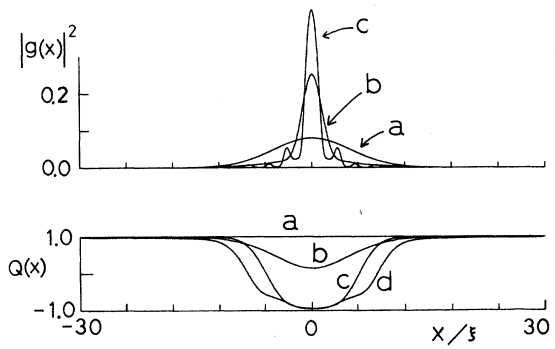


FIG. 7. $|g(x)|^2$ and $Q(x)$ at several typical $t$. No restriction is made on the form of $g(x)$. The frequency of the lattice vibration is $\omega=0.1\tau_0^{-1}$. (a) $t=0$, (b) $t=20\tau_0$, (c) $t=60\tau_0$, and (d) $t=100\tau_0$.

$Q(x)$, and we get an electron-lattice coupled oscillation. This oscillation will be referred to as an electron-lattice breather. It can be thought of as a bound state of $S^{e\text{-}l}$ and $\bar{S}^{e\text{-}l}$. In the present simulation, however, $g(x)$ becomes quite delocalized and the spatial dependence of $\phi_j(x)$ becomes very weak when the large-amplitude oscillation of $Q(x)$ is formed. Thus $Q(x)$ oscillates alone while the electronic state stays always close to the ground state. But this decoupling of the electron and the lattice may be an artifact, since our approximation becomes worse when $g(x)$ is delocalized and/or $x$ dependence of $\phi_j(x)$ is weak, as can be seen from the following arguments. (i) In a coherent state like Eq. (3.7), the quantum fluctuation $d(x)=\langle[\hat{\phi}(x)-\langle\hat{\phi}(x)\rangle]^2\rangle$ is independent of $x$ and assumed to be the same as in the ground state. But when the $x$ dependence of $\phi_j(x)$ becomes weak, the $x$ dependence of $d(x)$ becomes important; for example, if $\phi_j(x)$ is independent of $x$ the potential $V(x)$ can depend on $x$ only if the $x$ dependence of $d(x)$ is taken into account. (ii) We used the same internal structure $\phi_j(x)$ for all values of the center-of-mass coordinate $z$; in a more-accurate treatment we should take account of the $z$ dependence of the $\phi_j(x)$. In the case that $Q(x)$ has a large spatial variation, neglect of this $z$ dependence is allowed only when $g(z)$ is well localized. Thus it is almost certain that the large-amplitude oscillation of $Q(x)$ we have found in the present approximation corresponds to nothing but the electron-lattice breather found in the adiabatic approximation. If we accept this assignment, we can say that when we start from relatively delocalized $g(z)$ there are two possible relaxation products of the $^1A_g$ exciton: the neutral soliton pair and the electron-lattice breather. But, as pointed out at the start of this section, the classical treatment of $Q(x)$ becomes worse when the initial width of $g(z)$ is large. Thus we cannot exclude the possibility that the formation of the electron-lattice breather is an artifact due to the classical treatment of $Q(x)$.

Before closing this section, we briefly discuss the relaxation of the triplet exciton ($S^e$ or $B^e_\uparrow$). In the present approximation the magnitude of the total spin is not conserved, while the $z$ component of the total spin is conserved. Thus, in order to avoid unphysical mixing with the ground electronic state, it is better to use the $S^e$ state as an initial state. We carried out the simulations using the assumption Eq. (3.24a) for $|\Psi(t)\rangle$, and always got an $S^{e\text{-}l}_\uparrow+S^{e\text{-}l}_\uparrow$ pair as the relaxation product. There is no other channel of relaxation of the triplet exciton.

## VI. PHOTORELAXATION SCENARIO AND MORE ON ELECTRONIC SOLITONS

We showed in Sec. V that the $^1A_g$ excitation promptly decays into a neutral soliton pair ($S^{e\text{-}l}_\uparrow+S^{e\text{-}l}_\downarrow$) or their bound state (diradical breather, $B^{e\text{-}l}_{\uparrow\downarrow}$). In Fig. 8 the relaxation pathways to generate $S^{e\text{-}l}_\uparrow+S^{e\text{-}l}_\downarrow$ and $B^{e\text{-}l}_{\uparrow\downarrow}$ are shown. We use the symbols $S^{e\text{-}l}_\uparrow$, $S^{e\text{-}l}_\downarrow$, and $B^{e\text{-}l}_{\uparrow\downarrow}$ in order to distinguish them from charged solitons $S^{e\text{-}l}_+$ and $S^{e\text{-}l}_-$ and zwitterionic breather $B^{e\text{-}l}_{+-}$. $B^{e\text{-}l}_{\uparrow\downarrow}$ is a bound state of $S^{e\text{-}l}_\uparrow$ and $S^{e\text{-}l}_\downarrow$ and $B^{e\text{-}l}_{+-}$ is a bound state of $S^{e\text{-}l}_+$ and $S^{e\text{-}l}_-$.[8] Both $B^{e\text{-}l}_{\uparrow\downarrow}$ and $B^{e\text{-}l}_{+-}$ are localized, large-amplitude, and time-dependent oscillations of electrons and lattice. The presence of such breather oscillations was numerically demonstrated in the SSH model[7] and in the PPP model.[8] In Refs. 7 and 8, lattice oscillation was treated classically with the adiabatic approximation. After the lattice motion is quantized, discrete numbers of $B^{e\text{-}l}_{\uparrow\downarrow}$ and $B^{e\text{-}l}_{+-}$ will be left. Energy spacings between these quantized breathers may be of the order of the energy of an optical phonon. Then, high-energy (low-binding-energy) $B^{e\text{-}l}_{\uparrow\downarrow}$ can decompose into $S^{e\text{-}l}_\uparrow$ and $S^{e\text{-}l}_\downarrow$ by absorbing phonons. On the other hand, colliding $S^{e\text{-}l}_\uparrow$ and $S^{e\text{-}l}_\downarrow$ can be trapped into $B^{e\text{-}l}_{\uparrow\downarrow}$. Thus $S^{e\text{-}l}_\uparrow+S^{e\text{-}l}_\downarrow$ and $B^{e\text{-}l}_{\uparrow\downarrow}$ can be mutually converted by emitting or absorbing phonons.

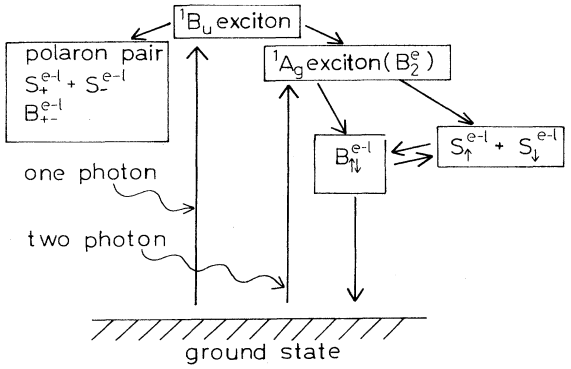


FIG. 8. Possible pathways of the photogeneration of a neutral soliton pair $S^{e\text{-}l}_\uparrow+S^{e\text{-}l}_\downarrow$ and of their bound state $B^{e\text{-}l}_{\uparrow\downarrow}$.

By one-photon absorption from the ground state, a $^1B_u$ exciton is created. Since this exciton is an ionic excitation, it can decay into $S^{e\text{-}l}_+ + S^{e\text{-}l}_-$ or a polaron pair. They have excess kinetic energy but would be quickly thermalized.[12] These charged excitations may be carriers of photocurrent. Neutral excitations (such as $^1A_g$ or $S^{e\text{-}l}_\uparrow$), on the other hand, can be created from $^1B_u$ exciton only through perturbations which break the electron-hole ($e$-$h$) symmetry.[10] If the one-photon absorption peak at 2.0 eV and the two-photon absorption peak at 1.8 eV are assigned to $^1B_u$ and $^1A_g$ excitons, respectively, the $^1B_u$-$^1A_g$ energy gap is small so that nonradiative transition is possible due to a weak perturbation breaking the $e$-$h$ symmetry. Grabowski *et al.*[11] suggested that the adiabatic energy surface of $^1B_u$ state does not fall off monotonically from the Frank-Condon state to the $S^{e\text{-}l}_+ + S^{e\text{-}l}_-$ state, but instead there is a local minimum in between them. If there is such a minimum, it is a candidate for the initial state of the transition to the $^1A_g$ state. In this way $S^{e\text{-}l}_\uparrow+S^{e\text{-}l}_\downarrow$ or $B^{e\text{-}l}_{\uparrow\downarrow}$ can be created by one-photon absorption through the $^1A_g$ state.

In the photoinduced absorption (PA) spectrum, the band which has a peak at 0.45 eV has been assigned to photogenerated charged solitons.[2,3] There is another PA band peaked at 1.35 eV.[1,2] This 1.35-eV band is regarded as due to the overall neutral excitations.[1,2] $B^{e\text{-}l}_{\uparrow\downarrow}$ is a possible candidate for the origin of this 1.35-eV band.[7,8] On one hand, Levey *et al.* observed the photoinduced ESR (PESR) signal by carefully eliminating the effect of transient heating.[6] Their PESR result suggests that neutral

solitons are photogenerated. Thus the relaxation paths shown in Fig. 8 can give a reasonable explanation for both the PA and PESR data.

There is a correlation between the excitation spectrum of the 1.35-eV PA band and the excitation spectrum of the PESR;[1,6] both the 1.35-eV PA and the PESR signals have stronger intensity when pumped by the red light than when pumped by the blue light. This is in sharp contrast with the 0.45-eV PA band and photocurrent;[1,3,4] they both have stronger intensity when pumped by the blue light than when pumped by the red light. Therefore it is natural to assume that neutral excitations $S^{e\text{-}l}_{\uparrow}$, $S^{e\text{-}l}_{\downarrow}$, and $B^{e\text{-}l}_{\uparrow\downarrow}$ are generated through a path different from that for generating charged excitations $S^{e\text{-}l}_{+}$, $S^{e\text{-}l}_{-}$, and $B^{e\text{-}l}_{+-}$. In the scheme shown in Fig. 8, the probability of decay from the $^1B_u$ to the $^1A_g$ state may be larger when pumped by the low-energy light, because the small $^1B_u$-$^1A_g$ energy gap makes the transition to the $^1A_g$ state easier. Consequently, the scheme that $S^{e\text{-}l}_{\uparrow}$, $S^{e\text{-}l}_{\downarrow}$, and $B^{e\text{-}l}_{\uparrow\downarrow}$ are generated via the $^1A_g$ state is consistent with the excitation spectrum of PA and PESR. Another possible process to generate $B^{e\text{-}l}_{\uparrow\downarrow}$ was studied by Bishop *et al.*[7] They showed $B^{e\text{-}l}_{\uparrow\downarrow}$ can be generated together with $S^{e\text{-}l}_{+}$ and $S^{e\text{-}l}_{-}$ directly from the $^1B_u$ excited state. This mechanism, however, does not explain the difference between the excitation spectrum of the 1.35-eV PA band and that of the 0.45-eV PA band.

Kivelson and Wu[13] proposed a different mechanism for the generation of $S^{e\text{-}l}_{\uparrow}$ and $S^{e\text{-}l}_{\downarrow}$. They showed the possibility that an almost-separate $S^{e\text{-}l}_{+}+S^{e\text{-}l}_{-}$ pair will decay into a $S^{e\text{-}l}_{\uparrow}+S^{e\text{-}l}_{\downarrow}$ pair due to the presence of a weak interaction which violates the electron-hole symmetry. It is not clear, however, whether this mechanism explains the excitation spectrum of PA and PESR. If ESR and absorption data induced by two-photon pumping are observed, the more detailed and direct information will be obtained to judge these theoretical models. If two-photon induced ESR and absorption have strong signals suggesting the generation of $S^{e\text{-}l}_{\uparrow}$, $S^{e\text{-}l}_{\downarrow}$, and $B^{e\text{-}l}_{\uparrow\downarrow}$, the importance of the decay process through the $^1A_g$ state may be certified.

Since the $^1B_u$ exciton is an ionic excitation, it cannot be described by our phase Hamiltonian Eq. (3.1). In order to study the relaxation process from the $^1B_u$ exciton to the $^1A_g$ state, charge and spin degrees of freedom must be treated on equal footing. This is possible by introducing two phase variables $\hat{\phi}$ and $\hat{\theta}$ which describe spin and charge degrees of freedom, respectively. Using this formalism, the PPP Hamiltonian can be transformed in the following form:[45]

$$H=\int dx[\,A_\rho(\nabla\hat{\theta})^2+C_\rho\hat{\pi}_\theta^{\,2}-B_\rho\cos(2\hat{\theta}) + A_\sigma(\nabla\hat{\phi})^2+C_\sigma\hat{\pi}_\phi^{\,2}+B_\sigma\cos(2\hat{\phi}) -2gu\cos\hat{\theta}\cos\hat{\phi}+(M/2a)\dot{u}^{\,2}+(2\kappa/a)u^2\,] , \tag{6.1}$$

where

$$[\hat{\theta}(x),\hat{\pi}_\theta(x')]=i\delta(x-x') ,$$
$$[\hat{\phi}(x),\hat{\pi}_\phi(x')]=i\delta(x-x') . \tag{6.2}$$

$u(x)$ is the lattice order parameter as in Eq. (3.1), and $g$ is an electron-lattice coupling constant. The explicit forms of the parameters $A_\rho$, $B_\rho$, $C_\rho$, $A_\sigma$, $B_\sigma$, and $C_\sigma$ can be found in Ref. 45. (They depend on the strength of the Coulomb interaction.) Local spin density $\hat{m}(x)$ and local charge density $\hat{n}(x)$ are related to $\hat{\phi}(x)$ and $\hat{\theta}(x)$ as

$$\hat{m}(x)=\frac{1}{2\pi}\nabla\hat{\phi}(x)-\frac{1}{a}\sin[2k_Fx+\hat{\theta}(x)]\sin\hat{\phi}(x) ,$$
$$\hat{n}(x)=\frac{1}{\pi}\nabla\hat{\theta}(x)+\frac{2}{a}\cos[2k_Fx+\hat{\theta}(x)]\cos\hat{\phi}(x) . \tag{6.3}$$

When the lattice is fixed at the uniformly dimerized configuration $[u(x)=u_0]$, $B_\rho$ and $B_\sigma$ terms can be neglected with respect to the term $V(\hat{\theta},\hat{\phi})=-2gu\cos\hat{\theta}\cos\hat{\phi}$ due to large quantum fluctuations.[36] Then it is easily seen that there are three types of electronic solitons which connect among the minima of the potential $V(\theta,\phi)$. For example, the electronic soliton connecting between $(\theta,\phi)=(0,0)$ and $(0,2\pi)$, which has spin 1 and charge 0, corresponds to the $^3B_u$ exciton. Besides these solitons, there may be some breathers. Classically, we can easily find two breathers. One is the $\phi$ breather in which $\theta$ is fixed at zero while $\phi$ oscillates just as Eq. (3.22). If the roles of $\theta$ and $\phi$ are interchanged, we get the $\theta$ breather. If these breathers survive the quantization procedure, we can make the following assignment; i.e., the $\phi$ breather corresponds to the $^1A_g$ exciton while the $\theta$ breather corresponds to the $^1B_u$ exciton. Whether this assignment is correct or not is now under study.

If the lattice has no dimerization ($u=0$), the Hamiltonian Eq. (6.1) decouples into two sine-Gordon Hamiltonians for $\hat{\theta}$ and $\hat{\phi}$. In this case the terms $\cos(2\hat{\theta})$ and $\cos(2\hat{\phi})$ cannot be neglected in general. The elementary excitations are given by the $\phi$ soliton and the $\theta$ soliton (both of them are $\pi$ kinks). If, however, the electron-electron interaction in the starting Hamiltonian Eq. (1.1) is a simple repulsive one, the energy of the $\phi$ soliton vanishes.[36] Thus $\phi$ solitons are created spontaneously, and the ground state can be regarded as a $\phi$-soliton liquid or as the so-called resonating valence-bond (RVB) state.[46] Then the $\phi$ soliton and the $\theta$ soliton should be related to the "spinon" and the "holon" excitations in the RVB state. To establish this relationship is also the subject of our current study.

In this paper, we discussed the electronic structure and dynamics of covalent excitons in polyacetylene using a nonperturbative method, i.e., the boson representation. Excitons are classified in terms of solitons and breathers. The solitonic character of the inner structure of excitons is the driving force of the lattice distortion. The Coulomb effects cannot be taken account of by simple renormalization of the parameters appearing in the SSH Hamiltonian. The nonlinearity of the Coulomb interaction manifests itself in the structure and dynamics of excited states in an explicit way.

## ACKNOWLEDGMENT

We thank the IMS computer center for the use of the HITAC S810 supercomputer.

## APPENDIX: GAUSSIAN OVERLAP APPROXIMATION

When $\beta$ is small the overlap $\langle z_1|z_2\rangle$ has a narrow peak at $z_1=z_2$, and it can be approximated by the following Gaussian:

$$\langle z_1|z_2\rangle \simeq e^{-\gamma(z_1-z_2)^2/2} , \tag{A1}$$

where $\gamma$, which is of order $\beta^{-2}$, is given by

$$\gamma=\frac{1}{\beta^2}\int dx\,dy\,D''(x-y)[q_0^2\phi_c(x)\phi_c(y)+\phi_c'(x)\phi_c'(y) +\pi_c(x)\pi_c(y)] , \tag{A2}$$

and $D(x-y)$ is the $\phi$-$\phi$ correlation function,

$$D(x-y)=\frac{1}{\beta^2}\langle\hat{\phi}(x)\hat{\phi}(y)\rangle=\frac{1}{2\sqrt{L}}\sum_k\frac{e^{ik(x-y)}}{(q_0^2+k^2)^{1/2}} . \tag{A3}$$

Here $L$ is the length of the system and the summation over $k$ is restricted to $|k|<k_c$, where the cutoff $k_c$ is taken to be $\pi/a$.

The energy expectation value $E=\langle\Psi|H|\Psi\rangle/\langle\Psi|\Psi\rangle$ can be evaluated within the Gaussian overlap approximation (GOA) (Ref. 44) as follows. Using the formula

$$\langle z_1|z_2\rangle\simeq\left[\frac{2\gamma}{\pi}\right]^{1/2}\int dz\,e^{-\gamma(z_1-z)^2}e^{-\gamma(z_2-z)^2} , \tag{A4}$$

we can express $\langle\Psi|\Psi\rangle$ and $\langle\Psi|H|\Psi\rangle$ as

$$\langle\Psi|\Psi\rangle=\left[\frac{2\gamma}{\pi}\right]^{1/2}\int dz\left|\int dz_1 e^{-\gamma(z_1-z)^2}f(z_1)\right|^2 , \tag{A5}$$

$$\langle\Psi|H|\Psi\rangle=\left[\frac{2\gamma}{\pi}\right]^{1/2}\int dz\,dz_1dz_2f^*(z_1)e^{-\gamma(z-z_1)^2} \times h(z_1,z_2)e^{-\gamma(z-z_2)^2}f(z_2) , \tag{A6}$$

where

$$h(z_1,z_2)=\langle z_1|H|z_2\rangle/\langle z_1|z_2\rangle . \tag{A7}$$

Within the GOA $h(z_1,z_2)$ can be approximated by its expansion around $z_1=z_2=z$ up to second order:

$$h(z_1,z_2)\simeq h(z)+\varepsilon_1h_1(z)+\varepsilon_2h_2(z) +\tfrac{1}{2}\varepsilon_1^2h_{11}(z)+\varepsilon_1\varepsilon_2h_{12}(z)+\tfrac{1}{2}\varepsilon_2^2h_{22}(z) , \tag{A8}$$

where $\varepsilon_j=z_j-z$ $(j=1,2)$, and

$$h(z)=\langle z|H|z\rangle , \tag{A9a}$$

$$h_1(z)=\left.\frac{\partial h(z_1,z_2)}{\partial z_1}\right|_{z_1=z_2=z} , \tag{A9b}$$

etc. In terms of the momentum operator $\hat{P}$ defined in Eq. (3.25), $h_1(z),h_{12}(z),\ldots$ can be expressed as

$$h_1(z)=i\langle z|\hat{P}H|z\rangle , \tag{A10a}$$

$$h_{12}(z)=\langle z|\hat{P}H\hat{P}|z\rangle-\gamma h(z) , \tag{A10b}$$

where $\gamma=\langle z|\hat{P}^2|z\rangle$ is identical to Eq. (A2). The following relations are also useful:

$$h_1'(z)=h_{11}(z)+h_{12}(z) , \tag{A11}$$

$$h''(z)=h_{11}(z)+2h_{12}(z)+h_{22}(z) , \tag{A12}$$

where a prime indicates differentiation with respect to $z$. Using the identities

$$\int dz_1f(z_1)e^{-\gamma(z_1-z)^2}(z_1-z)=\frac{1}{2\gamma}\partial f(z) , \tag{A13}$$

$$\int dz_1f(z_1)e^{-\gamma(z_1-z)^2}(z_1-z)^2=\frac{1}{4\gamma^2}(\partial^2+2\gamma)f(z) , \tag{A14}$$

where $\partial=\partial/\partial z$, and defining $g(z)$ by

$$g(z)=\mathcal{N}\int dz_1e^{-\gamma(z_1-z)^2}f(z_1) , \tag{A15}$$

where $\mathcal{N}$ is a normalization constant such that $\int dz|g(z)|^2=1$, we get the following expression for $E$:

$$E=\int dz\,g^*(z)\left[h(z)+\frac{1}{4\gamma}[\overleftarrow{\partial}(h_1-h_2) -(h_1-h_2)\overrightarrow{\partial}-2h_{12}] +\frac{1}{8\gamma^2}\overleftarrow{\partial}(4h_{12}-h'')\overrightarrow{\partial}\right]g(z) . \tag{A16}$$

To derive this equation, partial integrations and Eqs. (A11) and (A12) are used, and higher-order derivatives such as $h_{11}'$ are neglected to be consistent with the approximation in Eq. (A8). $h(z)$, $h_1(z)$, etc., can be evaluated by an elementary method, and we obtain

$$E=\int dz\,g^*(z)\mathcal{H}g(z) , \tag{A17}$$

where

$$\mathcal{H}=\overleftarrow{\partial}A_1(z)\overrightarrow{\partial}+i[\overleftarrow{\partial}W(z)-W(z)\overrightarrow{\partial}]+V_1(z) , \tag{A18}$$

and

$$A_1(z)=\frac{1}{2\gamma^2}A_0+\frac{vq_0^2}{8\gamma^2\beta^2}\int dx\,Q(x+z)(4\eta'^2\cos\phi_c-\phi_c''\sin\phi_c) , \tag{A19}$$

$$W(z)=\frac{vq_0^2}{2\gamma\beta^2}\int dx\,Q(x+z)\eta'(x)\sin\phi_c(x) , \tag{A20}$$

$$V_1(z)=\frac{v}{\beta^2}\int dx[\tfrac{1}{2}\phi_c'^2+\tfrac{1}{2}\pi_c^2-q_0^2Q(x+z)\cos\phi_c(x)]-\frac{1}{2\gamma}A_0-\frac{vq_0^2}{2\gamma\beta^2}\int dx\,Q(x+z)\cos\phi_c(x)(\tfrac{1}{4}\phi_c'^2+\eta'^2) , \tag{A21}$$

where

$$\eta(x)=\int dy\, D(x-y)\pi_c(y)\ , \tag{A22}$$

$$A_0=\frac{v}{2\beta^2}\int dx[\phi_c''^2+\pi_c'^2+q_0^2(\tfrac{1}{2}\phi_c'^2-2\eta'^2)]\ . \tag{A23}$$

Now we turn to the evaluation of the term

$$T=\frac{i}{2}\frac{\langle\Psi|\dot{\Psi}\rangle-\langle\dot{\Psi}|\Psi\rangle}{\langle\Psi|\Psi\rangle}=T_1+T_2\ , \tag{A24}$$

where

$$T_1=\frac{i}{2\langle\Psi|\Psi\rangle}\int dz_1dz_2f^*(z_1)\dot{f}(z_2)\langle z_1|z_2\rangle+\text{c.c.}, \tag{A25}$$

$$T_2=\frac{i}{2\langle\Psi|\Psi\rangle}\int dz_1dz_2f^*(z_1)f(z_2)\langle z_1|\partial_t|z_2\rangle+\text{c.c.} \tag{A26}$$

Using Eqs. (A4) and (A15), $T_1$ can be transformed into

$$T_1=\frac{i}{2}\int dz[g^*(z)\dot{g}(z)-\dot{g}^*(z)g(z)] \tag{A27}$$

(terms containing $\dot{\gamma}$ are exactly cancelled). $T_2$ can be calculated as follows. First we evaluate $\partial_t|z\rangle$ as

$$\partial_t|z\rangle=e^{i\hat{P}z}\partial_te^{iG}|0\rangle=e^{i\hat{P}z}(i\dot{G}+\tfrac{1}{2}[\dot{G},G])e^{iG}|0\rangle\ . \tag{A28}$$

Then using $\langle z_1|\partial_t|z_2\rangle/\langle z_1|z_2\rangle$ in the place of $h(z_1z_2)$ and following the calculation from Eq. (A8) to (A23), we get

$$T_2=A_2\int dz\left|\frac{\partial g(z)}{\partial z}\right|^2+V_2\ , \tag{A29}$$

where

$$V_2=\frac{1}{2\beta^2}\int dx\left[\dot{\phi}_c\pi_c-\dot{\pi}_c\phi_c+\frac{1}{2\gamma}(\dot{\phi}_c\pi_c''-\dot{\pi}_c\phi_c'')\right], \tag{A30}$$

$$A_2=\frac{1}{2\gamma^2\beta^2}\int dx(\dot{\phi}_c\pi_c''-\dot{\pi}_c\phi_c'')\ . \tag{A31}$$

The Lagrangian $\mathcal{L}$ is given by $\mathcal{L}=T-E$, and using Eqs. (A17), (A24), (A25), and (A29), we finally get

$$\mathcal{L}=\frac{i}{2}\int dz[g^*(z)\dot{g}(z)-\dot{g}^*(z)g(z)]-\int dz\, g^*(z)\mathcal{H}_{\text{eff}}g(z)\ , \tag{A32}$$

where

$$\mathcal{H}_{\text{eff}}=\bar{\partial}A(z)\vec{\partial}+i[\bar{\partial}W(z)-W(z)\vec{\partial}]+V(z)\ , \tag{A33}$$

and

$$A(z)=A_1(z)+A_2\ , \tag{A34}$$

$$V(z)=V_1(z)+V_2\ , \tag{A35}$$

and $A_1(z)$, $A_2$, $V_1(z)$, and $V_2$ are defined in Eqs. (A19), (A31), (A21), and (A30), respectively, and $W(z)$ is defined in Eq. (A20).

---

*Present address: Materials Research Laboratory, Central Engineering Laboratories, Nissan Motor Co. 1 Natsushima-cho, Yokosuka 237, Japan.

[1]For a review, see J. Orenstein, in *Handbook of Conducting Polymers,* edited by T. A. Skotheim (Dekker, New York, 1986).
[2]J. Orenstein and G. L. Baker, Phys. Rev. Lett. **49**, 1043 (1982).
[3]G. B. Blanchet, C. R. Fincher, T. C. Chung, and A. J. Heeger, Phys. Rev. Lett. **50**, 1938 (1983).
[4]L. Lauchlan, S. Etemad, T. C. Chung, A. J. Heeger, and A. G. Macdiarmid, Phys. Rev. B **24**, 3701 (1981).
[5]J. Orenstein, Z. Vardeny, G. L. Baker, G. Eagle, and S. Etemad, Phys. Rev. B **30**, 786 (1984).
[6]C. G. Levey, D. V. Lang, S. Etemad, G. L. Baker, and J. Orenstein, Synth. Met. **17**, 569 (1987).
[7]A. R. Bishop, D. K. Campbell, P. S. Lomdahl, B. Horovitz, and S. R. Philpott, Phys. Rev. Lett. **52**, 671 (1984).
[8]M. Sasai and H. Fukutome, Prog. Theor. Phys. **79**, 61 (1988).
[9]W. P. Su and J. R. Schrieffer, Proc. Natl. Acad. Sci. (U.S.A.) **77**, 5626 (1980).
[10]R. Ball, W. P. Su, and J. R. Schrieffer, J. Phys. (Paris) Colloq. **44**, C3-429 (1983).
[11]M. Grabowski, D. Hone, and J. R. Schrieffer, Phys. Rev. B **31**, 7850 (1985).
[12]S. Jeyadev and E. M. Conwell, Phys. Rev. B **35**, 5917 (1987).
[13]S. Kievelson and W.-K. Wu, Phys. Rev. B **34**, 5423 (1986).
[14]G. W. Hayden, and E. J. Mele, Phys. Rev. B **34**, 5484 (1986).
[15]H. Thomann, L. R. Dalton, Y. Tomkiewicz, N. S. Shiren, and T. C. Clarke, Phys. Rev. Lett. **50**, 533 (1983).
[16]S. Kuroda and H. Shirakawa, Phys. Rev. B **35**, 9380 (1987).
[17]T. C. Clarke and J. C. Scott, Solid State Commun. **41**, 389 (1982); M. Sasai and H. Fukutome, *ibid.* **51**, 609 (1984).
[18]I. Ikemoto, Y. Cao, M. Yamada, H. Kuroda, I. Harada, H. Shirakawa, and S. Ikeda, Bull. Chem. Soc. Jpn. **55**, 721 (1982); M. Sasai and H. Fukutome, Solid State Commun. **58**, 735 (1986).
[19]B. R. Weinberger, C. B. Roxolo, S. Etemad, G. L. Baker, and J. Orenstein, Phys. Rev. Lett. **53**, 86 (1984).
[20]W. P. Su, J. R. Schrieffer, and A. J. Heeger, Phys. Rev. Lett. **42**, 1698 (1979); Phys. Rev. B **22**, 2099 (1980).
[21]B. S. Hudson, B. E. Kohler, and K. Schulten, *Excited States* (Academic, New York, 1982), Vol. 6, p. 1.
[22]K. Schulten, I. Ohmine, and M. Karplus, J. Chem. Phys. **64**, 4422 (1976).
[23]P. Tavan and K. Schulten, J. Chem. Phys. **70**, 5407 (1979); **85**, 6602 (1986).
[24]I. Ohmine, M. Karplus, and K. Schulten, J. Chem. Phys. **68**, 2298 (1978).
[25]F. Kajzar, S. Etemad, G. L. Baker, and J. Messier, Synth. Met. **17**, 563 (1987).
[26]H. Fukutome and M. Sasai, Prog. Theor. Phys. **67**, 41 (1982); **69**, 1 (1983); **69**, 373 (1983).
[27]D. Baeriswil and K. Maki, Synth. Met. **17**, 13 (1987).
[28]D. K. Campbell, T. A. DeGrand, and S. Mazumdar, Phys. Rev. Lett. **52**, 1717 (1984).

[29]J. E. Hirsh and M. Grabowski, Phys. Rev. Lett. **52**, 1713 (1983).
[30]H. Hayashi and K. Nasu, Phys. Rev. B **32**, 5295 (1985).
[31]Z. G. Soos and L. R. Ducasse, J. Chem. Phys. **78**, 4092 (1983).
[32]K. Hashimoto, Int. J. Quantum Chem. **21**, 861 (1982); H. Fukutome and K. Hashimoto, Int. J. Quantum Chem. Symp. **15**, 33 (1981).
[33]H. Fukutome (private communication).
[34]L. N. Bulaevskii, Zh. Eksp. Teor. Fiz. **51**, 230 (1966) [Sov. Phys.—JETP **24**, 154 (1967)].
[35]S. Kuwajima, J. Chem. Phys. **74**, 6342 (1981); **77**, 1930 (1982).
[36]S. Tomonaga, Prog. Theor. Phys. **5**, 349 (1950); A. Luther, Phys. Rev. B **14**, 2153 (1976); J. Solyom, Adv. Phys. **28**, 201 (1979), and references therein.
[37]T. Nakano and H. Fukuyama, J. Phys. Soc. Jpn. **49**, 1679 (1980).
[38]J. Kondo, Physica B+C **98B**, 176 (1980).
[39]L. N. Bulaevskii, Zh. Eksp. Teor. Fiz. **43**, 968 (1962) [Sov. Phys.—JETP **16**, 685 (1963)]; **44**, 1008 (1963) [**17**, 684 (1963)].
[40]K. Hashimoto, Chem. Phys. **80**, 253 (1983).
[41]Y. Onodera and S. Okuno, J. Phys. Soc. Jpn. **52**, 2478 (1983).
[42]M. C. Cross and D. S. Fisher, Phys. Rev. B **19**, 402 (1979).
[43]R. F. Dashen, B. Hasslacher, and A. Neveu, Phys. Rev. D **11**, 3424 (1975).
[44]P.-G. Reinhard and K. Goeke, Rep. Prog. Phys. **50**, 1 (1987); P. Ring and P. Schuck, *The Nuclear Many-Body Problem* (Springer-Verlag, Berlin, 1980).
[45]J. Hara and H. Fukuyama, J. Phys. Soc. Jpn. **52**, 2128 (1983).
[46]P. W. Anderson, G. Baskaran, Z. Zou, and T. Hsu, Phys. Rev. Lett. **58**, 2790 (1987); S. A. Kivelson, D. S. Rokhsar, and J. P. Sethna, Phys. Rev. B **35**, 8865 (1987).